Structure and Dynamics of Colliding Plasma Jets

C. K. Li,[1] D. D. Ryutov,[2] S. X. Hu,[3] M. J. Rosenberg,[1] A. B. Zylstra,[1] F. H. Séguin,[1] J. A. Frenje,[1] D. T. Casey,[1]*
M. Gatu-Johnson[1], M. E. Manuel,[1†] H. G. Rinderknecht,[1] R. D. Petrasso,[1] P. A. Amendt,[2] H. S. Park,[2]
B. A. Remington,[2] S. C. Wilks,[2] R. Betti,[3] D. H. Froula,[3] J. P. Knauer,[3] D. D. Meyerhofer,[3]
R. P. Drake,[4] C. C. Kuranz,[4] R. Young,[4] and M. Koenig[5]

[1]*Plasma Science and Fusion Center, Massachusetts Institute of Technology, Cambridge, Massachusetts 02139 USA*
[2]*Lawrence Livermore National Laboratory, Livermore, California 94550 USA*
[3]*Laboratory for Laser Energetics, University of Rochester, Rochester, New York 14623 USA*
[4]*University of Michigan, Ann Arbor, Michigan USA*
[5]*Laboratoire pour l'Utilisation des Lasers Intenses, UMR 7605,*
CNRS–CEA–Université Paris VI–Ecole Polytechnique, 91128 Palaiseau Cedex, France

Monoenergetic-proton radiographs of laser-generated, high-Mach-number plasma jets colliding at various angles shed light on the structures and dynamics of these collisions. The observations are compared favorably with results from 2D hydrodynamic simulations of multi-stream plasma jets with collisional electrons and also with results from an analytic treatment of azimuthal magnetic field advection using a plausible model for velocity distribution of the effective electron flow. For collisions of two noncollinear jets, the observed flow structure is similar to the analytic model's prediction of a characteristic feature with a narrow structure pointing in one direction and a much thicker one pointing in the opposite direction. Spontaneous magnetic fields, largely azimuthal around the colliding jets and generated by the well-known $\nabla T_e \times \nabla n_e$ Biermann battery effect near the periphery of the laser spots, are demonstrated to be "frozen in" the plasma (due to high magnetic Reynolds number $R_M \sim 5\times10^4$) and advected along the jet streamlines of the electron flow. These studies provide novel insight into the interactions and dynamics of colliding plasma jets.

PACS numbers: 52.30.-q, 52.38.Fz, 52.72.+v

We report on recent experiments for studying the collisions of two identical plasma jets generated by high-power lasers. Modeled with comprehensive numerical simulations and analytic analysis, the measurements have, for the first time, indicated a key aspect of the jet collisions at various angles and the prediction of rapid expansion along the bisector plane, which agree with the analysis of frozen-in magnetic fields that were advected with streamlines of the plasma electron flow, reinforcing our insight into the interactions of colliding plasma jets.

The collision of high-Mach-number plasma jets in the laboratory is attracting increasing attention since such interactions can be used as an important test bed for studying many astrophysical phenomena and basic physics problems in self-organization [1-4]. Exploring the spatial structure and temporal evolution of these colliding jets, as well as their relationship with self-generated electromagnetic fields [5-8], is of essential importance for understanding the underlying physics of plasma jet interactions [9,10].

Although they have very different spatial, temporal, temperature and density scales, laboratory-generated plasma jets and astrophysical jets share a large variety of hydrodynamic similarities [11-18]. As indicated by numerous dimensionless parameters, these similarities suggest common physical processes that govern jet dynamics and allow us to scale laboratory jets to astrophysical conditions under some circumstances [9-18]. For example, recent experiments [2,3,19] and numerical simulations [20] indicate that the collisions of two counter-streaming plasma flows with sufficiently large spatial overlap lead to collisionless shocks mediated by the development of plasma micro-turbulence [21,22]. Such shocks can be scaled to mimic and explain many astrophysical phenomena [2-5, 9-22]. To simulate aspects of accretion disks and out-flows in astrophysics, an array of properly directed plasma jets has been proposed [23,24] to drive and form a differentially rotating, quasi-planar disc in which an azimuthal magnetic field, seeded with a cusp magnetic configuration, will be enhanced. The interactions among these jets in such a specially configured plasma will play a critical role in reproducing this particular astrophysical phenomenon [23,24]. In inertial confinement fusion (ICF) [25], the relevance of plasma jet interactions is evident in the plasma stagnation on a hohlraum axis (a consequence of radial collisions of supersonic high-Z wall blowoff), which is critical to hohlraum x-ray drive symmetry and ICF capsule implosions [25,26].

Laser-produced colliding jets can be supersonic [11-13, 27, 28], with sufficiently high kinetic energies that collisions of ions in one jet with ions in another jet are negligible. In this case, the ion streams interpenetrate each other essentially freely [1, 29]. On the other hand, the electrons (whose thermal velocity is much higher than the flow velocity) form a background common to both streams. As the electron temperature is lower than the ion directed energy by a factor ~ 50 - 100, they are highly collisional. The average velocity of the electrons is established to provide quasi-neutrality. For the case of equal strength streams the stagnation surface along which the magnetic flows from each plasma jet become parallel proves to be a plane which includes what would be the vector sum of the two equal flows and which would be

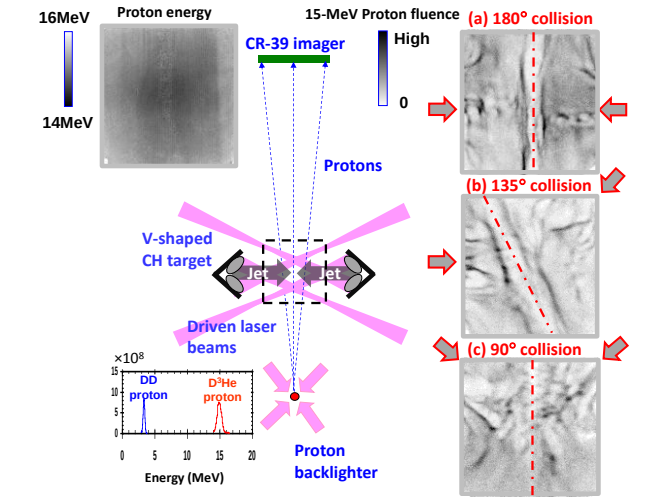

FIG 1. (Color online) Schematic diagram of the experimental setup. The proton backlighter (imploded D^3He-filled thin-glass-shell capsule driven by 30-OMEGA laser beams) is typically 1 cm from the collision region and has the illustrated monoenergetic spectra from the reactions $D + {}^3He \rightarrow \alpha + p$ (14.7MeV) and $D + D \rightarrow T + p$ (3.0 MeV). The typical backlighter spatial and temporal resolutions are ~ 40 μm and ~ 80 ps, respectively [42], and the relative timing between backlighter and V-shaped targets drive was adjusted to sample the jets' propagation and collision at a desired time. Sample radiographic images of proton fluence, taken with 15-MeV D^3He protons (the particle energies are slightly upshifted from the birth energies due to positive charging of the capsule) at ~ 4 ns from the onset of the laser drive on the V-shaped targets at different angles, are shown. The dash-dot lines shown in the images indicate the bisector planes for various cases. The dashed square indicates the field of view of the C39 proton detector, but shown as if it were rotated 90° into the plane of the diagram. The distance from the sample region to the detector is 27cm.

the bisector of the angle between the flows; this plane is therefore termed the "bisector plane." This picture cannot be adequately described by standard hydrodynamics. However, individual jets can be properly modeled by hydrodynamics [1, 29].

The experiments, illustrated schematically in Fig.1, were performed at the OMEGA Laser Facility [30]. V-shaped targets [31,32] were constructed with two 50-μm-thick, 3 mm × 3 mm plastic (CH) foils which have a full opening angle of 60º. Each foil was driven by two laser beams (0.351 μm in wavelength) at "angle ~ 28° to the foil normal towards the axis of the four-foil 2-beam set-up, with total energy ~ 1000 J during a 1-ns square pulse with full spatial and temporal smoothing [33]. A plasma plume was generated on each foil by laser ablation. When the plumes from the two adjacent foils collided they generated a plasma jet. The jet tip moving velocity is estimated using time-of-flight measurements to be V_j ~ 1700 km s^{-1}, indicating jet propagation is supersonic with internal Mach number M ~ 10 or greater after it has been traveling adiabatically for several nanoseconds. Two such jets, from two identical target pairs (distance between each target tip and the central collision region is 0.5 cm, collided with each other when they met at the bisector plane. Sample radiographic images, made with 15-MeV protons [34-36], for jet collisions at angles of 180°, 135° and 90°, are shown in Figs. 1 (a), (b) and (c), respectively.

A common and striking feature in these images is the "flattened" (quasi-planar) regions along the bisector planes, with proton fluence deficit shown inside but surplus protons on the edges. Plasma expansion perpendicular to the bisector plane is minimized because the plasma there reaches a balance between the continuous arrival of new jet material and the outflow of plasma along the bisector plane. Such a fluence structure must have resulted from deflections due to fields rather than plasma scattering. This is because the Coulomb scattering of these backlighting protons is negligible, since their energy loss while passing through the plasma is shown to be minimal by the proton energy image shown in Fig. 1 [37]. The apparently flattened, low-proton exposure region thus formed in the fluence images must be a consequence of proton deflection by fields on each side of the bisector plane with opposite directions. Such bisector features are clearly visible in proton images, indicating that the existence of this plane, together with the presence of the underlying symmetry of the magnetic field, is an unquestionable fact, irrespectively to fine details of the deflectometry theory. We note that the radiography method fortuitously gives strong contrast between the image feature associated with the bisector plane and the more subtle image features associated with the jet in the region between its source and the bisector plane. Away from the bisector plane, magnetic fields are nearly azimuthal around the jets and slowly varying with axial position; protons passing through this region experience deflection while approaching the jet that is nearly cancelled by an opposite deflection after passing the jet. Near the bisector plane, this cancellation does not occur because of rapid axial gradients and possibly chaotic structures. We also note that there is some angular spread in the directions of proton trajectories from the backlighter to the extreme edges of the imaged area, so the cancellations of deflections by the jets themselves, which is perfect only when the proton trajectory is almost perpendicular to the

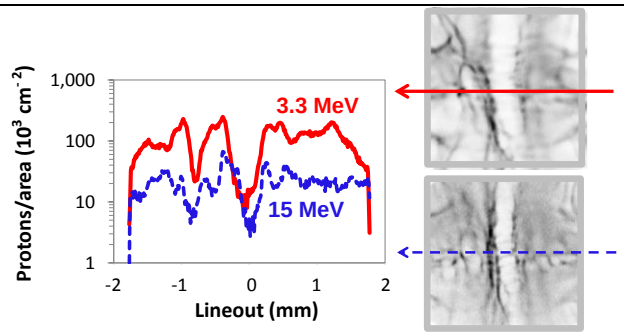

FIG. 2. (Color online) Lineouts from images taken at ~ 4.7ns with 15-MeV and 3.3-MeV protons from head-on collisions of two plasma jets are shown. The solid and dashed profiles correspond to the solid and dashed straight lines in the images, indicating the different energies of the backlighting protons. The ratio of the widths of the "flattened" region demonstrates the dominant role of magnetic field in forming such a structure.

jet direction, is not perfect across the full width of the image; however, any effect of angular spread would be gradual across the image and would not explain the stark difference between the apparent structures near the "bisector plane" and away from it.

Since there is azimuthal symmetry around the jet's axis, it is more convenient to first analyze the head-on collisions of two counter-streaming jets (Fig.1a). For uniquely determining the types of fields, Figure 2 gives lineouts crossing the flattened regions in the center of the images for two proton energies. The small-angle deflection is measured as the proton displacement in the detector plane (ξ) divided by the distance from plasma to detector (A-a). For deflection by electric fields, this is approximately equal to the ratio of the induced transverse velocity (the distance across the region divided by the injection velocity) to the injection velocity, which is proportional to the inverse of the proton energy ε_p^{-1}. By contrast, deflection by magnetic fields due to the Lorentz force [$\boldsymbol{F} = e\,(\boldsymbol{E} + \boldsymbol{v} \times \boldsymbol{B})$] is proportional to $\varepsilon_p^{-1/2}$. The ratio of the measured widths (FWHM) in this region for 3.3-MeV and 15-MeV protons is ~ 1.8, a number that is close to the square root of the proton energy ratio of (15 MeV/3.3 MeV)$^{1/2}$ ~ 2.1, strongly suggesting that the dominant source for proton deflections is magnetic fields rather than electric fields (15MeV/3.3MeV~ 4.6). These fields must have dominant azimuthal components (around the jet axis) and their strength is estimated by

$$\int \boldsymbol{B} \times d\ell = -\frac{A m_p V_p \xi}{q(A-a)a}\ , \qquad (1)$$

where a = 1 cm and A = 28 cm; m_p is proton mass and V_p is proton velocity; q is the proton electric charge and $d\boldsymbol{\ell}$ is the differential pathlength along the proton trajectory.

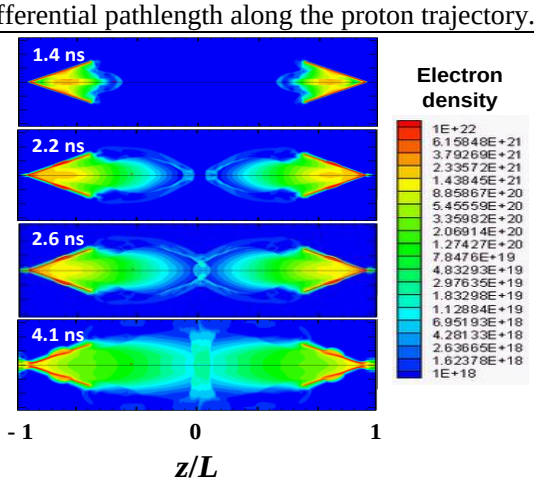

FIG. 3. (Color online) 2-D DRACO hydrodynamic simulations of the two head-on plasma jets which displays the jets' formation at $t \approx 1.4$ ns; propagation at $t \approx 2.2$ ns (a clear bow shock structure is seen in front of the jets); the onset of plasma flow in the transverse direction, and the formation of a high-pressure region in the bisector plane, at $t \approx 2.6$ ns; and the transverse expansion of the high-pressure region in the bisector plane $t \approx 4.1$ ns. In this simulation, a low density (~ 2×10^{-6} g cm^{-3}) deuterium gas has been added to the background. The simulation of plasma flow (4.1 ns) appears to be quite consistent with the shape of the proton deflection images shown in Figs. 1 and 2.

From Fig. 2, we obtain $|\int \boldsymbol{B}\times d\boldsymbol{\ell}|$ ~ 15 Tesla-cm. Taking the scale size as the diameter of the "flattened" disk (from a 3-D configuration) ≥ 0.5 cm (slightly larger than the field of view of our detector), results in a magnetic field roughly of order ~ 30 Tesla (T). Note that the magnetic deflection of the carbon and hydrogen ions of the streams has an opposite sign on the two sides of the bisector plane. For field weaker than ~ 30 T a mutual neutralization of the deflections may occur, restoring a simple conical ion flow in each of the jets.

The head-on collisions were simulated with the two-dimensional (2-D) hydrodynamic code DRACO (without self-generated magnetic field) [38,39]. Figure 3 displays post-processed snapshots showing the spatial structure and temporal evolution of two counter-streaming plasma jets colliding with each other. The morphology of the region of significant proton fluence modification corresponds remarkably well with the generic form of the magnetic-field spreading in the region of the bisector plane, which is supposed to correspond to the central region in Fig. 4(b). The DRACO simulation and Thomson scattering measurements [40] indicate that the electron "effective flow" stagnates in the axis and subsequently spreads sideways, forming a flattened region (a disk in 3-D view) with typical n_e ~ 10^{19}-10^{20} cm^{-3} and T_e ~ 500 – 1000 eV. This resembles the morphology of the model of Ref. [1] sufficiently closely as to suggest that their mechanism may indeed be the cause.

To place the discussions in the broader context of basic plasma physics, Table I gives physical parameters for the head-on collisions. The long jet-jet ion mean-free path indicates that the intra-jet ion-ion interactions are essentially collisionless. The general picture of the magnetic field being frozen into the electron fluid and advected along its streamlines is only to be expected if the magnetic Reynolds number is high, and indeed the estimated magnetic Reynolds number of Table 1 is gratifyingly large. Note that the carbon gyro-radius is comparable to or even smaller than the size of the observed structures, indicating that the regular azimuthal field may cause the ions to be deflected from their initial straight trajectories, create radial ion flow in both jets, significantly affecting the ion dynamics near the bisector-plane. This happens despite the fact that the magnetic pressure, p_M, of the 30 T field, as estimated from the measurements, is orders of magnitude smaller than the ram pressure, ρv^2, of either of the jets: $p_M/\rho v^2$ ~ 2×10^{-3}. The presence of the two counter-propagating streams makes this effect possible.

The generation and advection of spontaneous magnetic fields are described by the Faraday equation combined with a simplified version of the generalized Ohm's law: $\partial\boldsymbol{B}/\partial t = \nabla \times (\boldsymbol{u} \times \boldsymbol{B}) + \boldsymbol{S}$ [9] whose azimuthal component B_φ is given in cylindrical coordinate as

$$\frac{\partial B_\varphi}{\partial t} = \frac{\partial}{\partial r}\left(B_\varphi u_r\right) - \frac{\partial}{\partial z}\left(B_\varphi u_z\right) + S_\varphi\ , \qquad (2)$$

where u_r (u_z) is the radial (axial) component of the

TABLE I. Calculated parameters of two interpenetrating jets based on v = 1.7×10^8 cm s^{-1}; T_e ~ 1keV; n_C ~ 4×10^{18} cm^{-3} (per jet); length-scale of the overlap region L ~ 0.3 cm; and strength of magnetic field ~ 30 T.

Parameters	
Carbon ion energy (W_C)	175 keV
Carbon ion gyro-radius (r_G)	0.8 mm
Jet-jet ion mean-free path (λ_{ZZ})	20 cm
e-e collision frequency (ν_{ee})	3×10^{10} s^{-1}
Dynamic time ($t=l/v$)	1.75×10^{-9} s
Magnetic diffusivity (D_M)	10^3 cm^2 s^{-1}
Magnetic Reynolds number (Re_M)	5 ×10^4

velocity of effective electron flow [1], and S_φ is the source term for the field generation, which is dominated by the so-called Biermann battery effect due to the non-collinear gradients of electron density and temperature, in the form $\nabla n_e \times \nabla T_e$, with the fields evolving according to Eq. 2**.** The frozen-in condition for the azimuthal field in axisymmetric effective flow is [1]

$$B_\varphi / n_e r = const. \tag{3}$$

This suggests that there exists a zone near the bisector plane from which the plasma electron flow becomes almost radial, and the increasing plasma density due to contributions from the other jet would lead to the increase of magnetic fields as this flow spreads sideways, which is consistent with the observations (Fig. 1).

The streamlines of electron flow are modeled with the specific analytic process, as described in Ref [1], for head-on collisions. The streamlines of such electron flow are modeled with a solution of the differential equation in a cylindrical coordinates [1]

$$\frac{dr}{u_r} = \frac{dz}{u_Z}, \tag{4}$$

where the velocities u_r and u_z are giving by Eqs. (21) and (22) of Ref. [1], respectively. Near each target, the flow is diverging and the frozen-in Biermann battery field

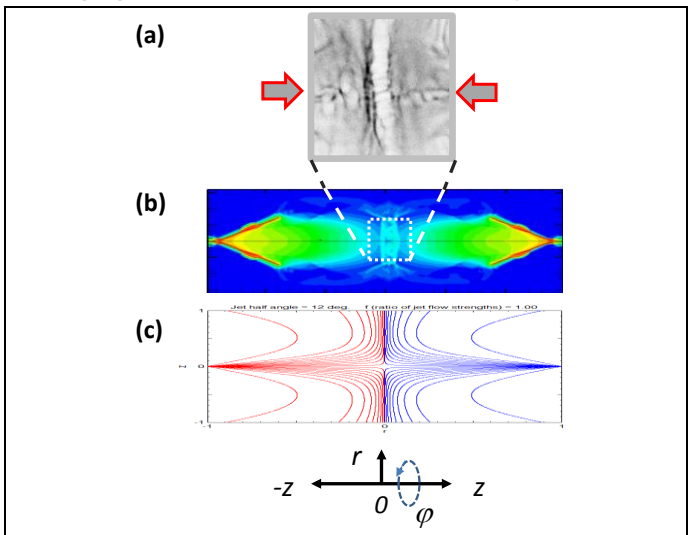

FIG. 4. (Color online) Proton image (a), numerical simulation (b), and analytical model (c) of streamlines of electron "effective flow" for collisions of two counter-streaming plasma jets (head-on).

decreases along the streamlines. Shown in Fig. 4 (c), the "conical" streamlines approach from both sides, stagnate and subsequently spread sideways, indicating the electron flow stagnates near the bisector plane, and the magnetic field is re-compressed to a quasi-planar structure [1,41]. The bisector plane acts as an impermeable boundary for electron fluid, and the re-compressed field has an opposite handedness in the opposite flows. By virtue of the frozen-in condition, the streamlines deviate toward much larger radii subsequent to the stagnation, leading to enhanced magnetic fields due to increasing products of density and radius (Eq. 3). These processes produce a"flattened" structure along the bisector plane and mimic the observed Fig. 4 (a) and simulated Fig. 4 (b) structure.

To model the noncollinear collisions at an arbitrary angle, a Cartesian coordinate system is more convenient because the azimuthal symmetry is broken [Fig. 5(a)]. Normalizing the distances to the parameter L (half-distance between the targets), an equation for the streamlines can be written:

$$\arctan\left(\frac{1}{\phi_1}\arctan\frac{y}{x}\right) - f\arctan\left(\frac{1}{\phi_2}\arctan\frac{x\sin 2\alpha + y\cos 2\alpha - 2\sin\alpha}{x\cos 2\alpha - y\sin 2\alpha - 2\cos\alpha}\right) = const. \tag{5}$$

where f is the ratio of the flow strengths of the two jets

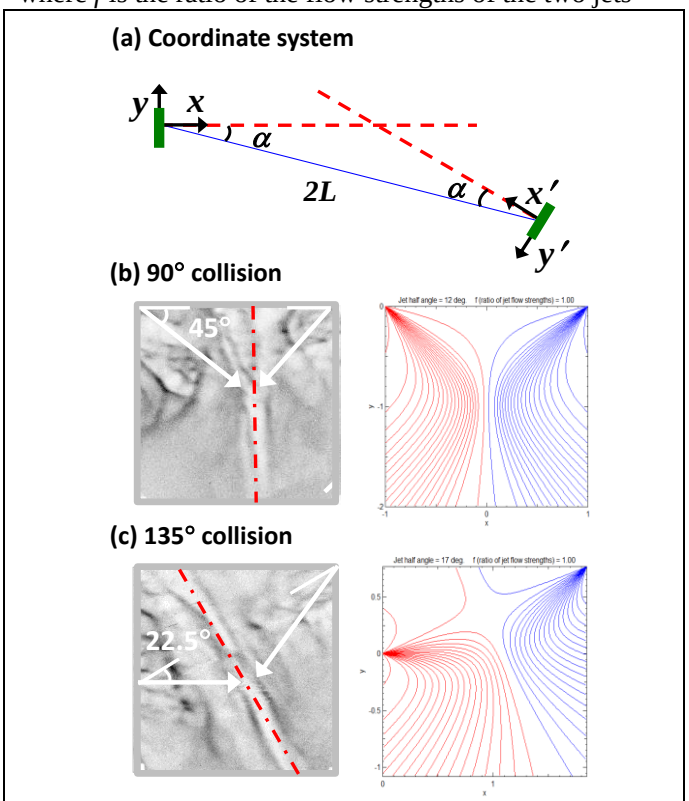

FIG. 5 (Color online) Schematic drawing of coordinate system (a) to illustrate the collisions of two plasma jets at an angle =180°-2α. Proton images of the collisions of two identical plasma jets (white arrows) is compared with model predicted streamlines of effective electron flow at 90° (α =45°) in (b) and 135° (α=22.5°) in (c), respectively. The dash-dot lines shown in the images indicate the bisector planes.

and ϕ_1 and ϕ_2 are the angular half-widths of the flows within the two jets. For 90° collisions where f =1, α = 45° and taking $\phi_1 = \phi_2 \approx 0.2$ radian (due to the jets being more collimated in these experiments), one obtains the streamline distribution shown in Fig. 5(b). The experimental proton image is well simulated, with a narrow structure pointing in one direction and a much thicker one pointing in the opposite direction in the bisector plane. This asymmetry is a consequence of collisions of tilted jets, which result in formation of stronger field compression (denser streamlines) in the forward direction and weaker in the backward direction. Although collisionality may increase somewhat due to a lower energy in the center-of-mass frame, the jets remain essentially collisionless. Figure 5(c) shows the experimental image and analytic streamlines for collisions of two equal colliding plasma jets collide at 135°(α= 22.5°).

The collisions of two noncollinear plasma jets are more generally relevant to those occurring in nature than collisions of perfectly collinear jets. For example, the asymmetric structures and dynamics of the collisions discussed above provide new insight into the jet-driven, differentially rotating quasi-planar disc in simulating accretion disks and out flows in astrophysics [23,24].

In summary, combining proton images with numerical simulations and analytic modeling we have systematically studied the structure and dynamics of collisions of two laser-generated, high-Mach-number plasma jets at different angles. Analyses of the measured characteristic features are strikingly consistent with the underlying physics of streamline distributions and demonstrate the advection of "frozen-in" spontaneous magnetic fields along the streamlines of electron flow. These studies provide novel physical insight into the interactions of two colliding plasma jets, and will be critical to the development of a unique test bed or platform for simulating frontier astrophysical phenomena and for addressing the basic physics of high-energy-density plasmas.

This work was supported in part by US DOE and LLE National Laser User's Facility (DE-FG52-07NA28 059 and DE-FG03-03SF22691), LLNL (B543881 and LDRD-08-ER-062), LLE (414090-G), and FSC at the U. of Rochester (412761-G).

∗ Now at Lawrence Livermore National Laboratory
† Now at the University of Michigan

[1] D. D. Ryutov *et al.*, Phys. Plasmas **20**, 032703 (2013).
[2] H. S. Park *et al.*, High Energy Density Phys. **8**, 38 (2012).
[3] N. L. Kugland *et al.*, Nature Phys. **8,** 809 (2012).
[4] J. M. Foster *et al.*, Phys. Plasmas 17, 112704 (2010).
[5] G. Gregori *et al*., Nature 481 480 (2012).
[6] S. Mondal *et al*., PNAS 109, 8011 (2012).
[7] H. Ahmed *et al*., Phys. Rev. Lett. 110 205001 (2013).
[8] M. Borghesi *et al*., Phys. Rev. Lett. 81, 112 (1998)
[9] R. P. Drake, *High-energy-density physics* (Springer, New York, 2006).
[10] B. A. Remington *et al.*, Rev. Mod. Phys. **78**, 755 (2006).
[11] D. R. Farley *et al.*, Phys. Rev. Lett. **83**, 1982 (1999).
[12] J. M. Foster *et al.*, Astrophys. J. **634**, L77 (2005).
[13] C. D. Gregory *et al.*, Plas. Phys. Contr. Fus. **50**, 124039 (2008)
[14] S. V. Lebedev, Astrophy. J. **616**, 988 (2004).
[15] P.A. Gourdain *et al.*, Phys. Rev. Lett. **110**, 015002 (2013).
[16] Ph. Nicolai *et al.*, Phys. Plasmas 17, 112903 (2010).
[17] D. D. Ryutov *et al.*, Astrophy. J. **127**, 465 (2000).
[18] D. D. Ryutov *et al.*, Phys. Plasmas **8**, 1804 (2001).
[19] S. Ross *et al.*, Phys. Plasmas, **19,** 056501 (2012).
[20] A. Spitkovsky Astrophys. J. **673**, L39 (2008).
[21] T. N. Kato *et al.*, Phys. Plasmas **17**, 032114 (2010).
[22] L. Gargate *et al.*, Astrophys. J. **744**, 67 (2012).
[23] D. D. Ryutov, Astrophys. Space Sci. **336**, 21 (2011).
[24] R. Young *et al.*, Bull. Am. Phys. Soc. **58,** ??? (2013).
[25] J. D. Lindl, Phys. Plasmas **2**, 3933 (1995).
[26] C. K. Li *et al.*, Science **327,** 1231 (2010).
[27] B. E. Blue, *et al.*, Phys. Rev. Lett. **95**, 095005 (2005).
[28] B. Loupias, *et al.*, Phys. Rev. Lett. **99**, 205001 (2007).
[29] D. D. Ryutov *et al.*, Phys. Plasmas **18**, 104504 (2011).
[30] J. M. Soures *et al.*, Phys. Plasmas **3**, 2108 (1996).
[31] K. Shigemori *et al.*, Phys. Rev. E. **962,** 8838 (2000).
[32] C. D. Gregory *et al.*, Astrophys. J. **676**, 420 (2008).
[33] D. D. Meyerhofer *et al*., Phys. Plasmas **8**, 2251 (2001).
[34] C. K. Li *et al*., Phys. Rev. Lett. 102 205001 (2009).
[35] M. Borghesi, *et al*., Rev. Sci. Inst. 74, 1688 (2003).
[36] L. Willingale *et al*. Phys. Plasmas 17, 043104 (2010).
[37] C. K. Li *et al.*, Phys. Rev. Lett. **70**, 3029 (1993).
[38] P. B. Radha *et al*., Phys. Plasmas 12, 056307 (2005).
[39] DRACO solves the two-dimensional radiation-hydrodynamic equation, assuming cylindrical symmetry. The electron-ion plasma is treated as a single fluid with separate electron and ion temperatures. Particle-collision effects are not included in the kinetic sense, and self-generated magnetic fields are not currently included in the simulations.
[40] M. J. Rosenberg *et al.*, Phys. Rev. E **86,** 056407 (2012).
[41] N. L. Kugland *et al.*, Phys. Plasmas **20**, 056313 (2013).
[42] C. K. Li *et al.*, Phys. Rev. Lett. **97**, 135003 (2006).